

Influence of Soil Type on the Structural Behavior of Reinforced Concrete Buildings with Elastomeric Anti-seismic Isolators

Leonel Suasaca Pelinco*, Junior Adolfo Perez Mendoza, Arnaldo Yana Torres, Efrain Parillo Sosa, Franz Joseph Barahona Perales

Faculty of Engineering and Sciences, Professional School of Civil Engineering, Universidad Andina Néstor Cáceres Velásquez, Peru

Received September 11, 2024; Revised November 26, 2024; Accepted December 23, 2024

Cite This Paper in the Following Citation Styles

(a): [1] Leonel Suasaca Pelinco, Junior Adolfo Perez Mendoza, Arnaldo Yana Torres, Efrain Parillo Sosa, Franz Joseph Barahona Perales, "Influence of Soil Type on the Structural Behavior of Reinforced Concrete Buildings with Elastomeric Anti-seismic Isolators," *Civil Engineering and Architecture*, Vol. 13, No. 1, pp. 716 - 732, 2025. DOI: 10.13189/cea.2025.130146.

(b): Leonel Suasaca Pelinco, Junior Adolfo Perez Mendoza, Arnaldo Yana Torres, Efrain Parillo Sosa, Franz Joseph Barahona Perales (2025). *Influence of Soil Type on the Structural Behavior of Reinforced Concrete Buildings with Elastomeric Anti-seismic Isolators*. *Civil Engineering and Architecture*, 13(1), 716 - 732. DOI: 10.13189/cea.2025.130146.

Copyright©2025 by authors, all rights reserved. Authors agree that this article remains permanently open access under the terms of the Creative Commons Attribution License 4.0 International License

Abstract The study's general objective was to analyze soil type's influence on the structural behavior of reinforced concrete buildings with elastomeric anti-seismic isolators. The study was treated with a quantitative approach, a non-experimental design of applied type, with a comparative scope, considering the object of study as category A1 buildings related to structures erected on soil profiles S1 and S3 and the sample as a dual structural system of category A (clinical) with the incorporation of an isolation interface, structure formed by 4 levels with soil factor type S1 and S3. The techniques used were the structural approach in the plan and height of the building and the use of software for modeling, correction, and scaling of earthquakes. Initially, static and dynamic seismic analysis was performed. As a result, it was obtained that the values of energy input to the structure and the values of dissipation or absorption of such energy by the HDRB isolation devices, allow a ratio between S3/S1 soils, which reaches values of up to 75%. Consequently, it is concluded that on S1 soil, HDRB isolators will make a better contribution and will dissipate a higher percentage of input energy; in addition, they will strengthen the seismic behavior of a type A1 building.

Keywords Structural Behavior, Reinforced Concrete, Elastomeric Insulators, HDRB Insulation, S1 and S3 Soils

1. Introduction

An unexpected adverse situation that a reinforced concrete structure may face is the deterioration and collapse due to the splitting of its structural and nonstructural components, caused by seismic loads [1]. In this sense, regardless of the type of facilities and the functions it fulfills, this observation represents a starting point to expose the disaster risks it represents for the survival of people [2].

In perspective, reinforced concrete, also called reinforced concrete, is called as such due to the proportional composition of reinforced steel in its conformation [3]. It has been used since 1954 thanks to the contribution generated by William Wilkinson, who presented and patented it in that decade [4]. Since then, it has been evolving according to the needs and requirements of the construction industry and, in addition, to the research and development of safe structures, which are complemented by systematic studies of soil types [5], to diagnose the conditions that must be addressed and thus guarantee a reliable resistance to the effects of adverse

events resulting from seismic movements [6, 7].

In this order of ideas, to infer with a certain degree of accuracy the behavior of the soil located under urban structures such as houses, shopping centers, and hospitals, among others, built with reinforced concrete in the face of tectonic plate movements, it is possible to achieve the simulated configuration of seismic spectra with different magnitudes [8]. For this purpose, several digital technological resources or modeling or simulation programs are available, among which is the Etabs V. 20.0.0 student version [9].

In perspective, Etabs V. 20.0.0.0 is a structural engineering software that allows the analysis and design of multilevel structures. It includes modeling templates and load prescriptions based on the various international design codes. In addition, it allows the representation of basic and advanced systems in both static and dynamic conditions, becoming a tool of great impact on data processing during the development of a project [10]. Similarly, the resulting data will be processed using Microsoft Excel.

As a starting point, the type or profile of the soil where the structure under study is to be located must be specified. In that sense, profiles in soils, such as S1 and S3, can be an important starting point for setting a decision criterion [11]. The S1 profile is characterized by the conformation of rocks or very stiff soils with wave propagation velocities or shear force \bar{V}_s , between 500 m/s and 1500 m/s, while the S3 profile is associated with soft soils, which are identified by being very flexible, with shear wave propagation velocities \bar{V}_s , less or equal to 180 m/s [12], considering the Technical Standard Seismic Resistant Design E.030, Chapter IV [13]. Similarly, the geophysical characteristics and conditions of the soil profiles can be specified as shown in Table 1, as well as equation (1), to determine the shear strength.

Table 1. Floor profiles according to standard E-030-2016

Profile	V_s	N_{60}	S_u
S ₀	>1500 m/s	-	-
S ₁	Between 500 m/s and 1500 m/s	>50	>100 kPa
S ₂	Between 180 m/s and 500 m/s	Between 15 and 50	Between 50 kPa and 100 kPa
S ₃	<180 m/s	<15	Between 25 kPa and 50 kPa
*S ₄			

Extremely flexible soil, according to the Mechanical Soil Study (MSE), V_s , average concrete wave velocity, N_{60} weighted average of the standard penetration test and S_u weighted average of the shear strength in undrained condition.

$$V = (Z * U * C * S/R) * P \quad (1)$$

Where:

Z: Gravity acceleration fraction

U: Usage factor

C: Seismic amplification factor

S: Shear strength

R: Basic coefficient of seismic force reduction

P: Weight of the structure

In any case, $C/R \geq 0,125$

Another significant aspect of determining and analyzing the structural behavior of buildings is the vibration period. This is variable and depends especially on the type of soil on which the structure is supported [14]. Thus, a building founded on rock or rigid soil generates a response similar to a cantilever perfectly embedded in the base and, therefore, will show a lower vibration period. However, if it is on soft soil, the vibrations will generate an evident deformation, because the soil-building assembly becomes more flexible and the period increases, behaving as if it were partially coupled as a result of the deformation of the embedment [15].

Considering the type of soil, its association with the period of vibration, and the seismic spectrum, the determination of the structural behavior of a given building under seismic loads can begin, where the fundamental period of vibration, the maximum displacements, and the correlation between the significant modes are evaluated [16, 17, 18]. Within this approach, another aspect that is considered with great attention is structural stiffness. To counteract its presence during a seismic movement, technological resources that are strategically adapted between the structure and the foundation are currently employed, which are known as elastomeric anti-seismic isolators [19, 20, 21, 22]. Their main function is to dampen and absorb movement, and to counteract the generation of deformations in the event of an earthquake [23, 24].

Although it is true that recent studies have evaluated the structural behavior of buildings, very few of these studies have gone deeper into the observation of the reaction to seismic loads of structures with foundations isolated by means of elastomeric devices. Consequently, the purpose of the present study is to analyze the influence of soil type on the structural behavior of reinforced concrete A1 buildings with elastomeric anti-seismic isolators.

In this context, it is necessary for the team of professionals in the construction and urban planning sector to have prior information on the type of soil on which an urban structure is planned to be erected, such as multilevel buildings for residences, hospitals, schools, among others; this is an important preliminary step to estimate control parameters in the design. However, having means, mechanisms and devices that significantly isolate the foundations from potential seismic movements represents a preventive measure of great impact. Therefore, the installation of elastomeric isolators at the base of such structures will be a very important step [17].

It is equally important to be able to use standard data on simulated cases with projected structures, to estimate and infer the behavior of a given structure before it is erected, with the use of specialized *software* and algorithms

developed for that purpose [9-10]. This is part of the relevance and pertinence of the development of this study.

The starting point of the study is the following question: what is the influence of soil type on the structural behavior of A1 reinforced concrete buildings with elastomeric anti-seismic isolators? In this sense, the execution of the present study ratifies the importance of knowing the type of soil, which is a determining factor in the structural design, and is also a basic criterion for the selection, installation, and adjustment of the isolation mechanisms between the structure and the ground in case of earthquakes.

In this order of ideas, elastomeric anti-seismic isolators are special devices, whose properties allow optimizing the design to improve the safety and resilience of reinforced concrete buildings. If they are correctly selected for their maximum use, the impact of seismic movements can be mitigated. The results of this study, it is expected to make a significant contribution to engineering professionals and the scientific community with relevant data on the previous management of soil profiles and the use of elastomeric isolators in type A1 structures, to mitigate potential seismic loads and favor the preservation of the structure.

2. Literature Review

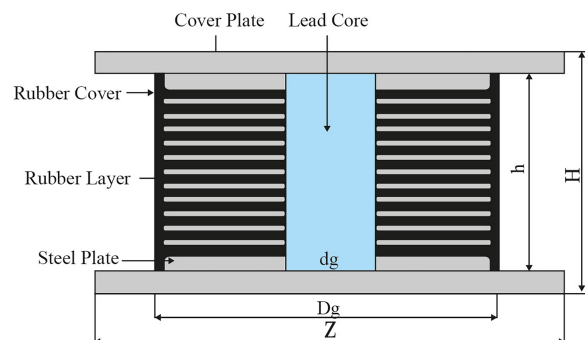
First, reference is made to soil profiles and their designation s_1 , s_2 , s_3 , and s_4 , considering the approach of the E-03 standard by [13]. For this, soil profiles are classified considering the average shear wave propagation velocity, or alternatively for granular soils, the weighted average of the N_{60} , obtained by a standard penetration test (SPT), or the weighted average of the shear strength in undrained condition (s_u) for cohesive soils. They are estimated in these properties, considering the upper 30 m of the soil profile, delimited from the level of the foundation bottom, as indicated in numeral 2.3.2. In relation to the use of methods and techniques for the isolation of structures, it is indicated that referring to neoprene supports, which as a structure has a lead core that increases initial stiffness and dissipates energy during earthquakes, according to Noggle and Van Engelen [25]. In addition, the inclusion of a rubber core in an infinite band of reinforced steel is considered to enhance the function of the elastomeric isolator. Furthermore, a solution was developed based on a hypothetical pressure solution including and excluding the compressibility of neoprene for compression and bending properties.

An economical alternative, which fits the needs of developing countries, for the isolation of structures against eventual seismic loads (FREI) according to Pianese et al. is presented [19]. This alternative is to use (PBFREI) to adhere the reduced area of the rubber device to the

connecting steel. PBFREI retains beneficial characteristics of both bonded and unbonded applications, such as improved lateral plasticity and hoist intransigence and sliding forces. To facilitate fabrication and installation, as well as the possibility of unbonded fiber reinforced isolator (UFREI) applications, the authors propose a FREI made of high cushioning gum and glass fiber fabrics. Performance can be examined under bonded conditions and in partially adhered and unadhered applications.

Considering the contribution of Yenidogan [26], who performed a historical analysis of the various technologies for the isolation of structures to cope with seismic loads, elastomeric isolation devices can be classified into three main categories according to their damping and composite material properties. In the European standard EN 15129, a device called “polymer plug rubber bearings (PPRB)” is included, along with three main elastomeric bearings. Low-damping elastomeric isolators (LDRB) are composed of natural rubber, steel wedges and end plates. High- and low-damping rubber bearings have a similar configuration.

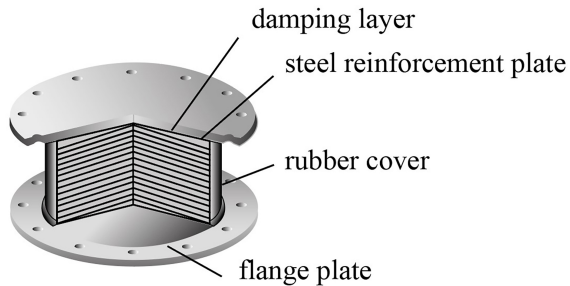
It should be noted that elastomeric isolators are the most widely used devices to achieve stable restoration of the structure in cases of seismic motion [27]. These are constructed with natural rubber material, which offers a high level of damping, flexibility, and strength to counteract potential negative effects in multilevel reinforced concrete structures [28]. Figure 1 shows a lead core elastomeric bushing (LRB) currently in use.



Note. Ziraoui et al. [29].

Figure 1. Representation of a high-damping elastomeric isolator LRB

Similarly, Figure 2 shows the representation of the High Damping Rubber Bearing (HDRB) elastomeric isolator. This is characterized by having a special composition that dissipates seismic energy due to its deformation and heat generation. Under standard conditions, it functions as a standardized deformation support, so it is specially designed for structures with limited space, where it is very difficult to install separate support and seismic protection systems.



Note. Rafik and Abdelhak [30].

Figure 2. Representation of an HDRB high-damping elastomeric isolator

However, the in-depth study of the soil type is of great importance, because according to its characteristics, the seismic wave travels in a certain direction, with specific velocity and acceleration [31]. From this perspective, the structural behavior of the building depends directly on the static and dynamic load, as well as on the geometry and the construction material (strength, stiffness and ductility), so it is a point of attention of great importance when guaranteeing the integrity and permanence of the building [32].

In this order of ideas, facilities such as public or private health facilities categorized as A1, are at high risk due to their scope of accommodation for patients and staff. Therefore, it is imperative to ensure their functionality during and after a seismic event [13]. In a specific context, within this type of building, the medical equipment, as well as the totality of facilities, have the same level of importance that is equated with the infrastructure itself, all this due to its high economic value.

3. Materials and Methods

3.1. Type of Study, Population, and Sample

The study was treated with a quantitative approach, a non-experimental design of applied type, with a comparative scope, considering the object of study (category A1 buildings) related to structures erected on S1 and S3 soil profiles. A dual structural system of category A (clinical) with the incorporation of an isolation interface, a structure formed by 4 levels with soil factor type S1 and S3, was set as a sample.

3.2. Research Techniques

The techniques used were the structural plan and height of the building and the use of software for modeling,

correction, and scaling earthquakes. Initially, the embedded structure is subjected to static and dynamic seismic analysis [33, 34] to determine whether it complies with the parameters required by the Technical Standard E-030 Seismic Resistant Design, chapter IV [13].

Once the corresponding parameters were verified, we proceeded with the isolation interface and its respective devices, determining their mechanical physical properties, comparing, and ensuring these values with the Tensa company's catalog for the structure isolated with HDRB-type devices.

3.3. Procedure

The time-history (T-H) analysis [35] was developed with records of the Pisco (Ica) earthquake in 2007 [36], which were corrected and scaled using seismic engineering software, SeismoMatch, and SeismoSignal software. To emulate the behavior of the building, the Etabs V. 20.0.0.0 student version software was used for the corrections and scaling of the accelerograms [37, 38].

In this order of ideas, the influence or relationship between the S1/S3 soils was verified to obtain the seismic response of the study sample [36, 37], by incorporating HDRB base isolators where the planned results were achieved. In addition, the energy was dissipated by the devices for both soils, concluding in the influence that the type of soil has on the structural behavior of the building [38].

A dynamic spectral analysis was performed considering a series of parameters estimated based on the soil profiles as shown in Table 2.

Table 3 summarizes the characteristics and nominal properties of the HDRB isolation devices.

As explained, the general objective of this study was to analyze the influence of soil type on the structural behavior of reinforced concrete buildings with elastomeric seismic isolators. For this purpose, the following questions were developed: what will be the level of the structural response of the building when a seismic isolation system is implemented according to the type of soil, and what will be the percentage of influence of the isolators for energy dissipation according to the type of soil?

In this regard, a specific case was taken as a 4-level dual structural system built for health category A1 (private clinic) with a roofed area equal to 720 m² and lengths of 36 meters on the x-x axis and 24 m on the y-y axis; it includes circulation, stairs and central elevator of the building, with soil factor type S1 and S3, using as technical support of the standards E.030 Seismic Resistant Design of the National Building Regulations [13] and E.031 Seismic Isolation of the National Building Regulations [39].

Table 2. Parameters for dynamic analysis of the structure

Nomenclature	Acronym	Soil factor	
		S1	S3
Zone	Z3	0.35	0.35
Use	U	1.00	1.00
Seismic coefficient	C	2.50	2.50
Soil factor	S	1.20	1
Reduction factor	R	7.00	7.00
Period defining the C-factor platform	Top	0.40	1.00
Period defining the beginning of the C-factor zone with constant displacement	T _I	2.50	1.60
Period X-X direction	T _X	0.4614	0.4614
Period Y-Y direction	T _Y	0.3184	0.3184
Fixed seismic-B reduction factor	R	7	7
Isolated seismic-B reduction factor	R	1	1
Reduction factor seismic superstructure	R	2	2

Table 3. Nominal properties of HDRB isolation devices

Type of insulator according to location	Unit	Type A device	Type B device
Design load	Tn	133.94	66.97
Tensa Catalog		TDRI-500-NM-154	TDRI-450-NM-150
Vertical (U1)			
Vertical stiffness (<i>effective stiffness</i>)	KN/mm	791	693
Linear Properties (U2, U3)			
Effective linear stiffness (<i>effective stiffness</i>)	KN/mm	1.02	0.85
Effective Cushioning (<i>effective damping</i>)	kn. seg/mm	0.09	0.08
Non-linear properties (U2, U3)			
Initial stiffness (<i>stiffness</i>)	KN/mm	8.04	6.70
Fluency strength (<i>yield strength</i>)	kn	72.22	60.18
R.I nic/R. ratio. Post	ratio	0.096	0.096
Energy Dissipated	Kn.m	66.17	55.14
Post creep stiffness	KN/mm	0.77	0.64

4. Results

4.1. Modeling Procedure and Structure Analysis

A 4-story dual structural system building for health category A1 (private clinic) with a roofed area equals 720 m² and lengths of 36 m on the x-axis and 24 m on the y-axis, including stairway circulation and central elevator of the building. Figure 3 shows the simulation of the structure in question. Etabs 2020 V1 *software* was used for seismic analyses. To mimic the behavior of the analyzed structure,

previously calculated data were assigned, such as preliminary dimensioning and specific weights, load assignment, design spectra, and seismic acceleration records reported by the Peruvian Japanese Center for Seismic Research and Disaster Mitigation (CISMID - UNI).

Table 4 shows the seismic record for the case study considering the Pisco earthquake in Ica in 2007.

SeismoSignal *software* was used for the correction of the accelerograms, and SeismoMatch *software* was used for the amplification of the target earthquake. Data processing

and analysis will be performed using Excel software. The HDRB-type isolator from the Tensa catalog was used, complying with our previous calculations on the physical and mechanical properties of the isolator. Figure 4 shows the correction of the seismic records, which avoids the

deviation of the accelerogram, correcting the frequency components caused by movements or noises foreign to the isolator.

Similarly, the target seismic spectrum graph is presented as shown in Figure 5.

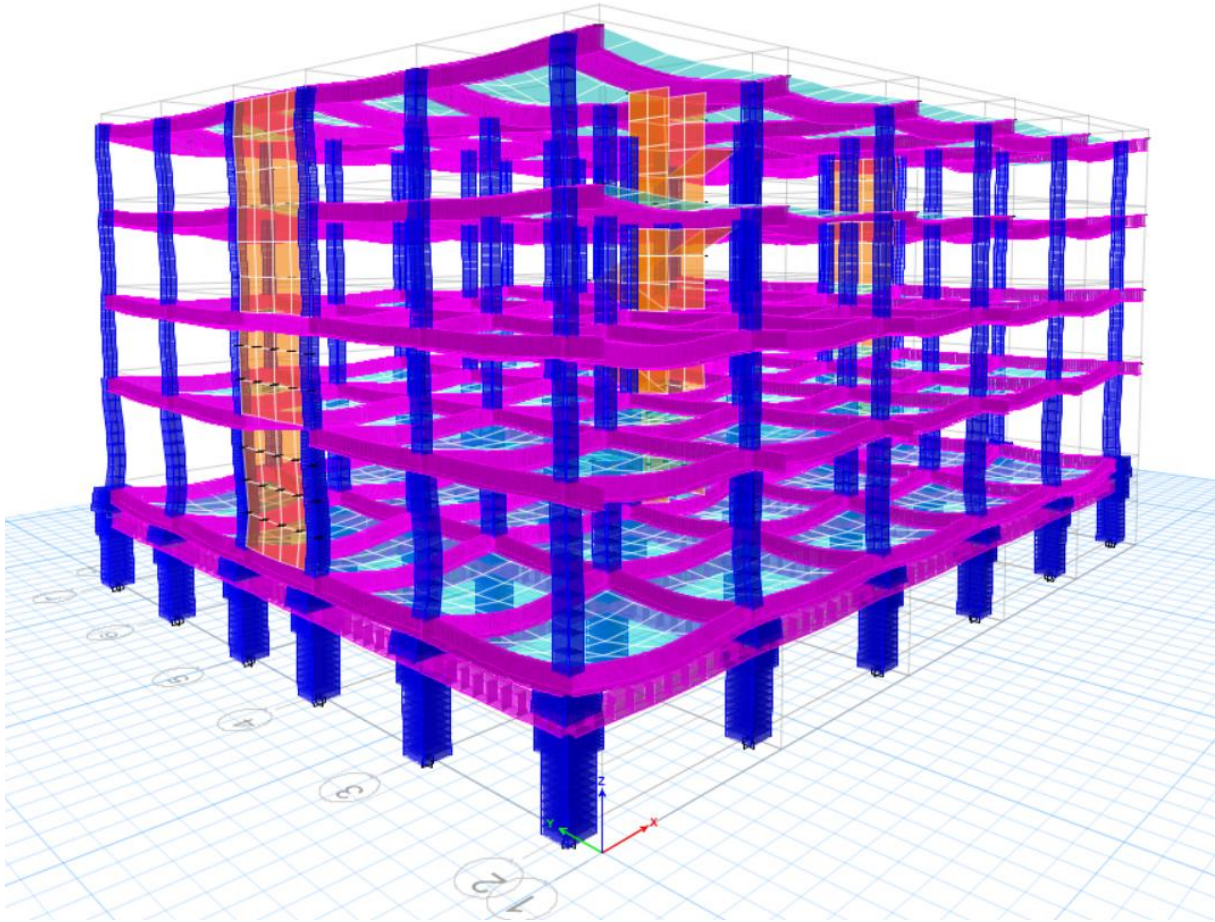
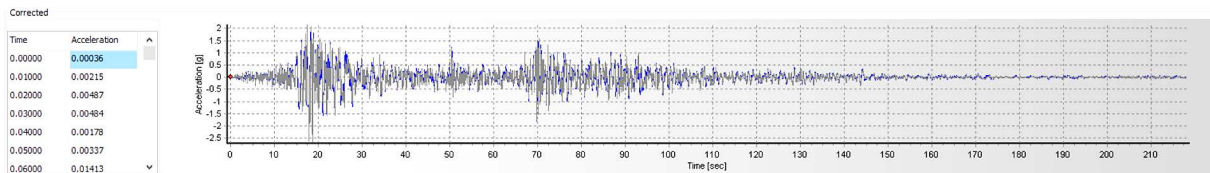


Figure 3. Structure designed with fixed base and isolation interface

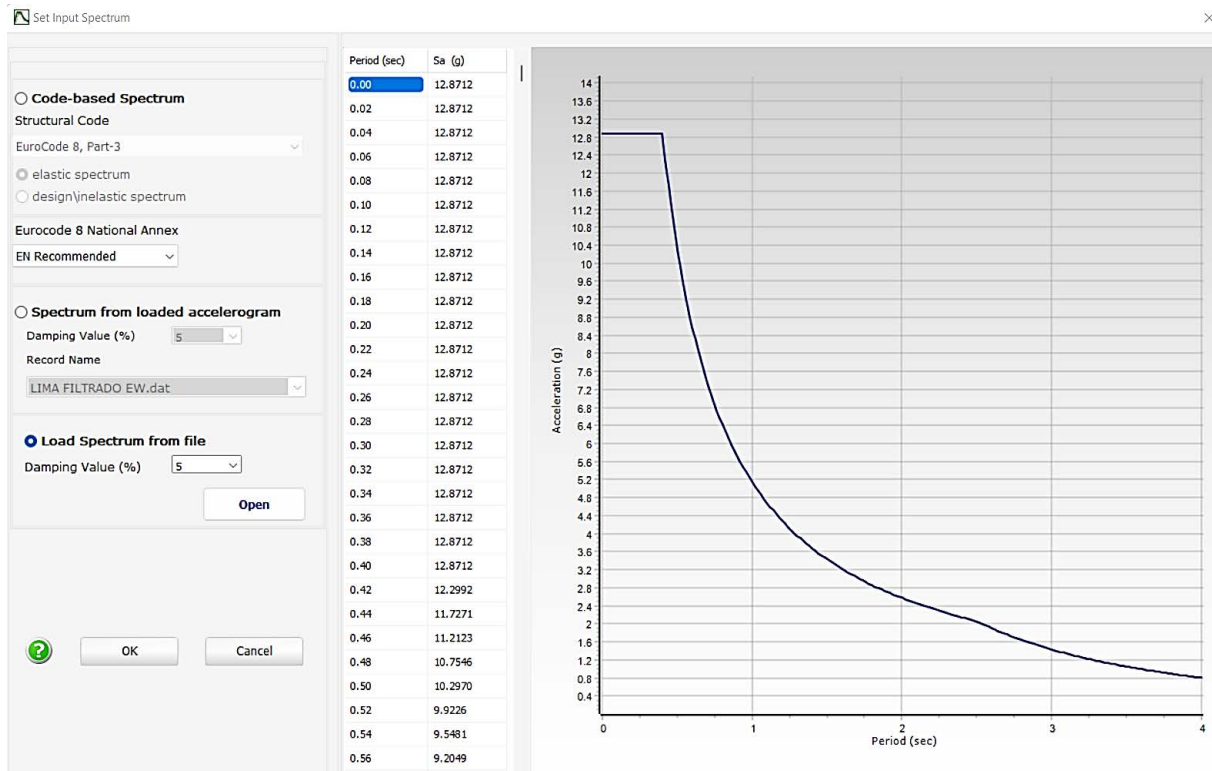
Table 4. Ica-2007 seismic record

Seism	Station Location	Date	Magnitude of the earthquake	Max Acceleration -cm/S2 EW	Max Acceleration -cm/s2 NS
Ica	San Luis Gonzaga National University, Ica, Ica	August 15/2007	7.9	-272.82	333.66



Note. Seism Signal 2021

Figure 4. Corrected accelerogram-Ica_2007- EW



Note. Seism Match 2023

Figure 5. Target seismic spectrum

4.2. Definition of Criteria for Structure Emulation

For concrete

1. $F'c = 280 \text{ MPa}$
2. $E = 15000 \times \text{SQR}(280) \times 10 = 2509980 \text{ Ton/m}^2$
3. Poisson $U = 0.2$
4. Weight per unit volume = $2,4 \text{ Ton/m}^3$

For steel

5. $F'y = 4200 \text{ MPa}$
6. $E = 2 \times 10^6 \text{ kg/cm}^2 = 2000000 \text{ MPa}$
7. Weight per unit volume = $7,849 \text{ Ton/m}^3$

Load Factors

100 % CM + 50 CV + 25 %CVT

4.3. Vibration Period, Participative Mass, and Shear Strength

First, to estimate the response level, the vibration period of the structure was configured, considering the fixed base (without the isolators) against the isolated base. In this sense, technical aspects of a seismic-resistant design were considered to obtain an inelastic response with an adequate performance against an earthquake under specifications similar to those of Ica 2007. Figure 6 shows the expected results considering three specific modes.

Figure 6 shows the increase of the vibration period for the structure with isolation at the base, which complies with the design philosophy of isolated structures, for fixed base $t = 0.461 \text{ sec.}$ and isolated base $t = 2.033 \text{ sec.}$,

considering an influence of 77 %. Regarding the mass participation in the Fixed Base vs. Isolated Base X-X & Y-Y system, Table 5 shows the components involved according to the model.

Table 5 shows the participation of masses in more than 90% of the first three vibration modes of the structure with an isolated base, which is recommended by the E-030 standard. Regarding the base shear force V_s or basal shear force, it is the one that vectorially carries a direction and sense perpendicular (X-axis) to the base of the structure built vertically (Y-axis). It results from the product of spectral acceleration and the mass of the building. Figure 7 shows the determination of the basal shear force in the X-X direction.

Figure 7 shows the V_{sx} to which the structure with a fixed base and with an isolated base is subjected for the 2 types of soil proposed. It also shows the influence between them with a maximum value of V_s at the base of the structure with a fixed base equal to 27% and with the isolated base of up to 58%, in the X-X direction of analysis. Similarly, Table 6 shows the shear forces but in the Y-Y direction.

Table 6 shows the V_{sy} to which the structure with fixed base and with isolated base is subjected for the 2 types of soil proposed; it also shows the influence between them with a maximum value of V_s at the base of the structure with fixed base equal to 17% and with isolated base of up to 58%, in the Y-Y direction of analysis.

VIBRATION PERIOD - (FIXED BASE VS ISOLATED BASE)

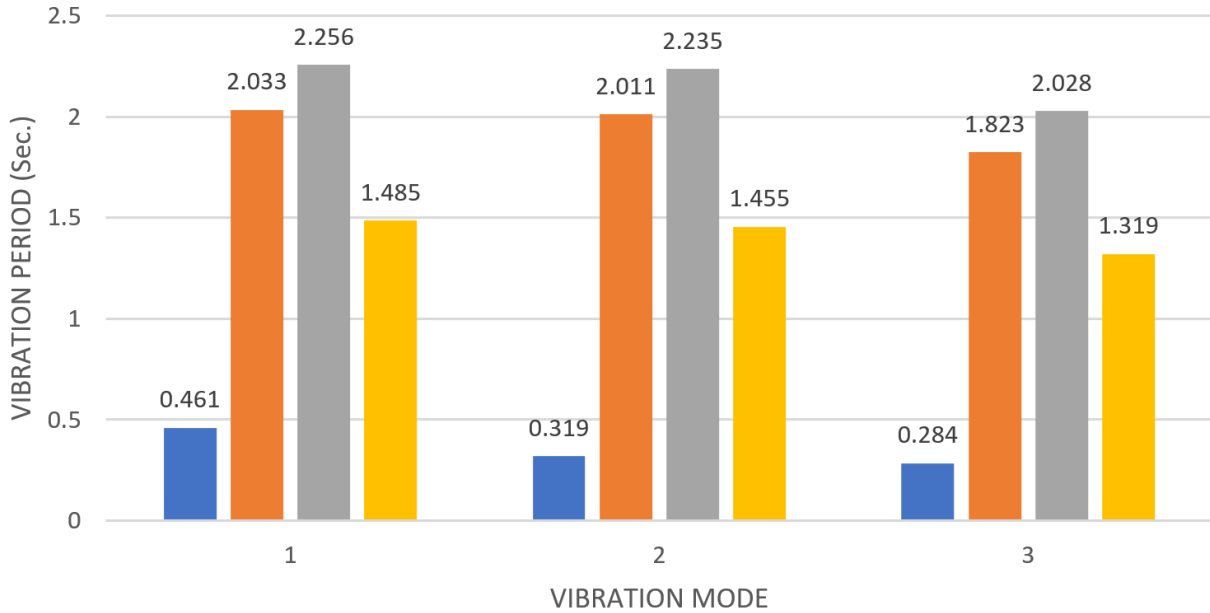


Figure 6. T - fixed base vs. isolated base P.N - L.I & L.S

Table 5. Participating mass according to vibration modes fixed base vs. isolated base

Participating mass-fixed base vs. isolated base													
Case	Mode	Fixed Base			Isolated Base P. N			Insulated base L. I			Isolated Base L. S		
		Period sec	Sum UX	Sum UY	Period sec	Sum UX	Sum UY	Period sec	Sum UX	Sum UY	Period sec	Sum UX	Sum UY
Modal	1	0.461	85%	0%	2.033	93%	0%	2.256	93%	0%	1.485	92%	0%
Modal	2	0.319	85%	79%	2.011	93%	94%	2.235	93%	94%	1.455	92%	94%
Modal	3	0.284	85%	79%	1.823	94%	94%	2.028	94%	94%	1.319	93%	94%

INFLUENCE OF SOIL TYPE (S1/S3) SHEAR FORCES Vx

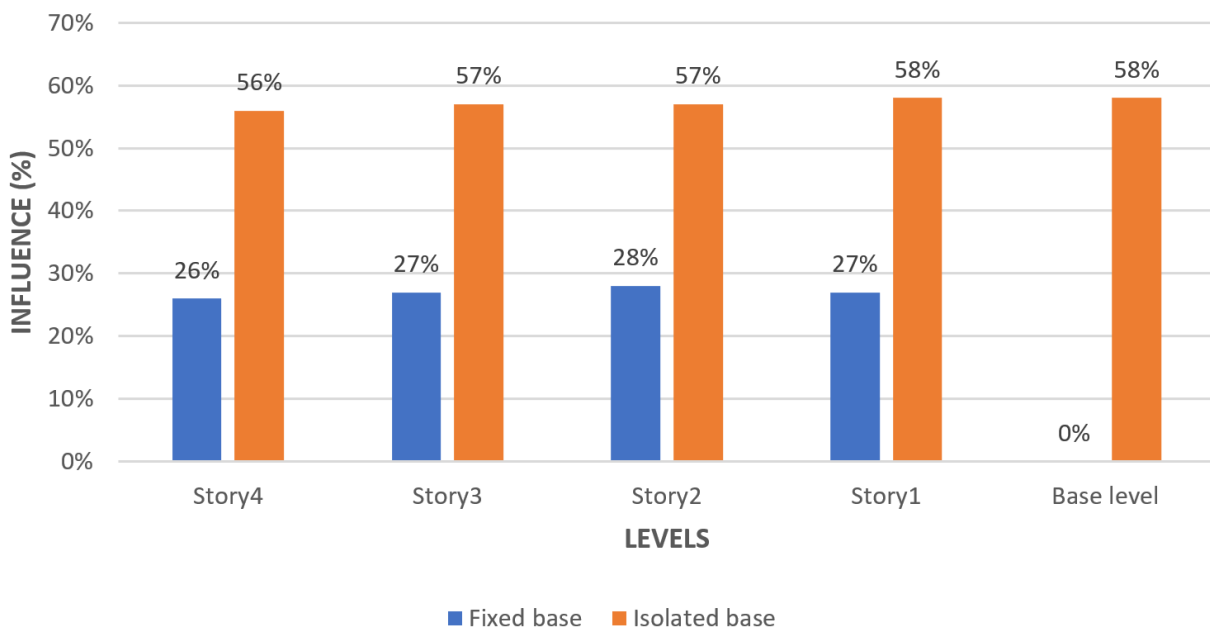


Figure 7. Vs - SMC R=2 (Z3- S1 VS Z3 - S3) X-X Direction

Table 6. V_s - SMC R=2 (Z3- S1 VS Z3 - S3) Y-Y Direction

SMC R=2 Y-Y DIRECTION										
Description		Z3-S1			Z3-S3			S1/S3		S1/S3
Story	Case	Fixed Base	Isolated Base	Fixed B. / Isol. B.	Fixed Base	Isolated Base	Influence			
		V_y	V_y	Influence	V_y	V_y	Fixed Isol. B.	B./ Fixed B.	Isol. B.	
		(TN)	(TN)	%	(TN)	(TN)	%	%	%	
4	SMC R=2Y-Y	358.73	32.64	91%	430.44	75.83	82%	17%	57%	
3	SMC R=2Y-Y	821.20	94.11	89%	985.38	221.39	78%	17%	57%	
2	SMC R=2Y-Y	1115.37	153.84	86%	1338.35	364.74	73%	17%	58%	
1	SMC R=2Y-Y	1279.78	214.10	83%	1535.63	510.14	67%	17%	58%	
Base	SMC R=2Y-Y		283.44			676.61				

4.4. Displacements

Next, the maximum displacement is determined in both X-X (Figure 8) and Y-Y (Table 7) directions.

Figure 8 shows the maximum displacements that the structure with a fixed base and with an isolated base will suffer for the two types of soil, as well as the influence between them with a maximum value of displacement at the base of the structure with a fixed base equal to 28% and with the isolated base of up to 57%, in the X-X direction of analysis.

Table 7 shows the maximum displacements that the structure with a fixed base and with an isolated base will suffer for the two types of soil, as well as the influence between them with a maximum value of displacement at the base of the structure with a fixed base equal to 17% and with the isolated base of up to 58%, in the Y-Y direction of analysis.

4.5. Time-history Analysis (T-H)

Another fundamental aspect of the study is the time-history (T-H) analysis. The E-031 standard was considered, for the Ica_2007_EW case, first in the X-X direction and then Y-Y in the corresponding cases in the

types of soils studied. Tables 8, 9, 10, and 11 show the information collected on relative lateral displacement between two adjacent floors of a building.

For the structure with an isolated base for an earthquake of ICA_2007_EW, the minimum and maximum drift values were obtained. The isolated structure with soil type S1 has a maximum drift value at the first level equal to 0.0018 and for S3 equal to 0.0034, where the influence of the relationship between soil types S1/S3 is 47% in the X-X direction. Likewise, for the Y-Y direction with soil type S1, it reaches a maximum value at the first level equal to 0.0013 and for S3 equal to 0.024, where the influence of the relationship between soil types S1/S3 is 46 % in the Y-Y direction.

For the structure with an isolated base for an earthquake of ICA_2007_NS, the minimum and maximum drift values were obtained. The isolated structure with soil type S1 has a maximum drift value at the first level equal to 0.0016 and for S3 equal to 0.0038, where the influence of the relationship between soil types S1/S3 is 59% in the X-X direction. Likewise, for the Y-Y direction a soil type S1 reaches a maximum value at the first level equal to 0.0005 and an S3 equal to 0.0026, where the influence of the relationship between soil types S1/S3 is 81 % in the Y-Y direction.

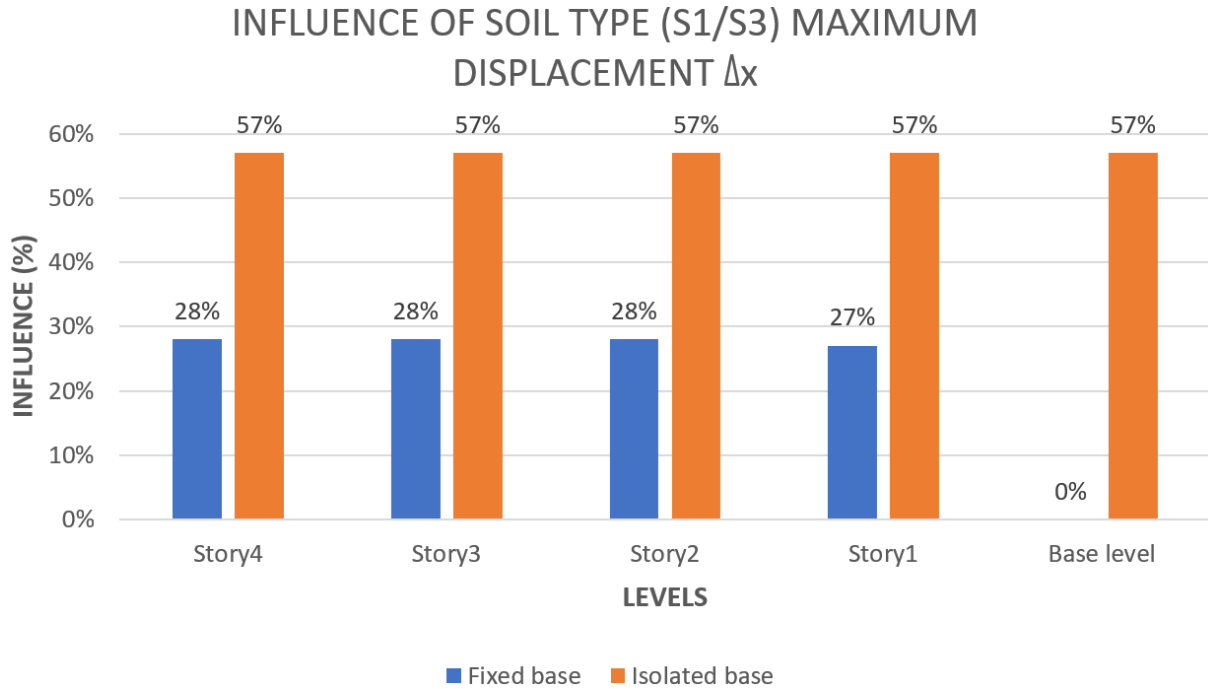


Figure 8. Maximum displacement SMC R=2 (Z3- S1 VS Z3 - S3) X-X

Table 7. Maximum displacement SMC R=2 (Z3- S1 VS Z3 - S3) Y-Y

Description		R=2 DIRECTION Y-Y								
		Z3-S1		Z3-S3			S1/S3		S1/S3	
Story	Elevation	Location	Fixed B.	Isola. B.	Fixed B. / Isola. B.	Fixed B.	Isol. B.	Fixed B. / Isol. B.	Fixed B.	Isola. B.
			Y-Dir	Y-Dir	Influence	Y-Dir	Y-Dir	Influence	Influence	Influence
		cm	cm	cm	%	cm	cm	%	%	%
Story4	3	Top	2.84	10.45	73%	3.41	24.95	86%	17%	58%
Story3	3	Top	2.04	10.29	80%	2.45	24.57	90%	17%	58%
Story2	3	Top	1.27	10.12	87%	1.53	24.15	94%	17%	58%
Story1	4	Top	0.56	9.92	94%	0.67	23.68	97%	17%	58%
BASE LEVEL	0	Top		9.66	100%		23.07	100%		58%
Maximum displacement last level/base			2.285	0.7886	65%	2.742	1.880	31%	17%	58%

Table 8. Drifts-direction X-X - Ica_2007_EW - S1/S3

DRIFTS (X Sense)				Ica Case 2007 XX-EW.				
Description		Z3-s1		Z3-s3		S1/s3	Drift Max.	Control
Level	Diaphragm	UX (m)	D. Inelastic	UX (m)	D. Inelastic	Influence %	E-031	E-031
Story4	D4	0.1723	0.0006	0.3766	0.0015	56%	0.005	√
Story3	D3	0.1704	0.0011	0.3722	0.0024	55%	0.005	√
Story2	D2	0.1672	0.0015	0.3650	0.0032	52%	0.005	√
Story1	D1	0.1626	0.0018	0.3554	0.0034	47%	0.005	√
Base	DETAILS	0.1554		0.3418	0.0000			

Table 9. Drifts - Y-Y Direction - Ica_2007_EW - S1/S3

DRIFTS (Y Sense)						Ica Case 2007 YY-EW		
Description		Z3-s1		Z3-s3		S1/s3	DriftMax.	Control
Level	Diaphragm	Uy (m)	D. Inelastic	Uy (m)	D. Inelastic	Influence%	E-031	E-031
Story4	D4	0.1745	0.0011	0.3729	0.0021	48%	0.005	√
Story3	D3	0.1713	0.0012	0.3667	0.0023	46%	0.005	√
Story2	D2	0.1676	0.0013	0.3599	0.0025	47%	0.005	√
Story1	D1	0.1636	0.0013	0.3525	0.0024	46%	0.005	√
Base level	DETAILS	0.1585		0.3429				

Table 10. Drifts - X-X Direction - Ica_2007_NS - S1/S3

DRIFTS (Y Sense)						Ica Case 2007 XX-NS		
Description		Z3-s1		Z3-s3		S1/s3	DriftsMax.	Control
Level	Diaphragm	Ux (m)	D. Inelastic	Ux (m)	D. Inelastic	Influence %	E-031	E-031
Story4	D4	0.1160	0.0008	0.4238	0.0018	53%	0.005	√
Story3	D3	0.1134	0.0014	0.4184	0.0029	53%	0.005	√
Story2	D2	0.1093	0.0016	0.4098	0.0037	56%	0.005	√
Story1	D1	0.1045	0.0016	0.3986	0.0038	59%	0.005	√
Base level	DAILS	0.0982		0.3834				

Table 11. Drifts - Y-Y Direction - Ica_2007_NS - S1/S3

DRIFTS (Y Sense)						Ica Case 2007 YY-NS		
Description		Z3-s1		Z3-s3		S1/s3	DriftMax.	Control
Level	Diaphragm	Uy (m)	D. Inelastic	Uy (m)	D. Inelastic	Influence %	E-031	E-031
Story4	D4	0.1038	0.0003	0.4282	0.0022	88%	0.005	√
Story3	D3	0.1030	0.0003	0.4218	0.0024	88%	0.005	√
Story2	D2	0.1022	0.0004	0.4145	0.0027	85%	0.005	√
Story1	D1	0.1010	0.0005	0.4065	0.0026	81%	0.005	√
Base level	DAISL	0.0990		0.3962				

4.6. Acceleration of Mezzanine Floors

Another important parameter in this study is represented by the inter-story acceleration $SD_R=7$, taking into account the type of soil. With this information, the dynamic response of the structure during an earthquake is estimated. Therefore, the acceleration experienced by each floor of the building concerning the other floors and the

base during a seismic event is determined. Table 12 summarizes the results obtained for this study.

The values shown in Table 12 show the influence of soil type for maximum acceleration that will reach the structure, where the ratio between them, S1/S3, considering the isolated base structure, will have a maximum value (at level 1) equal to 58% in the X-X direction and 57% in the Y-Y direction of analysis.

Table 12. Influence of floor-to-floor acceleration - design earthquake R=7 - S1/S3

DESIGN FLOOR_SEISMIC ACCELERATION R=7 GROUND - S3							
Description		Fixed Base S3		Isola. Base S3		Influence	Influence
LEVEL	CASE	XX	YY	XX	YY	Isola.B./Fixed B. X-X	Isola. B./Fixed B. Y-Y
		g	g	g	g	%	%
4	SiS_DIN_XX Max	0.0195	0.0212	0.0431	0.0444	55%	52%
3	SiS_DIN_XX Max	0.0178	0.0178	0.0418	0.0414	57%	57%
2	SiS_DIN_XX Max	0.0170	0.0171	0.0407	0.0404	58%	58%
1	SiS_DIN_XX Max	0.0167	0.0174	0.0397	0.0401	58%	57%
BASE	SiS_DIN_XX Max	0.0168	0.0167	0.0354	0.0389	53%	57%

4.7. Hysteretic Loop Analysis and Distribution of DRB-type Isolators

Figure 9 shows the distribution of the HDRB-type seismic isolators, according to Standard E-031 [43]. The isolation devices are in the K6 and K26 corners of the structure because they have different mechanical characteristics, considering the characteristics and records of the earthquake in Ica, Peru, 2007.

The diagram in Figure 9 shows the reference point or cut-off point between the X and Y axes in the lower left corner, where the similarity with a Cartesian axis can be appreciated. The structure is then subjected to a simulation with the records of the Ica-2007 earthquake. If the peak ground acceleration is increased, in successive steps, we proceed with an incremental dynamic analysis. These procedures are applied to the structure, considering the following: in the first, the values of the control parameters are used as they come in the *software*, which are *default* values; in the second, the values determined by the calibration procedure are used. Tables 13 and 14 show the results obtained.

When simulating a case like that of Ica-2007_EW, the HDRB isolator (K6 - corner), we have for the S1 soil a $\Delta = 15.87$ cm, in the X-X direction, for the Y-Y direction, a $\Delta = 16.42$ cm. However, for soil S3 with the Ica_2007_EW earthquake a $\Delta = 33.17$ cm in the X-X direction, while for the Y-Y direction a $\Delta = 33.65$ c. Likewise, the influence between each other (S1/S3) for the X-X direction reaches a reduction percentage of up to

52 % and for the Y-Y direction, the influence between each other reaches a reduction percentage of up to 51 % in the Y-Y direction. For point K-26, for a soil type S1 in the X-X direction, a $\Delta = 16.77$ cm is reached, and in Y-Y a $\Delta = 16.65$ cm. When considering soil S3, in the X-X direction a $\Delta = 34.39$ cm is reached, and in Y-Y a $\Delta = 34.08$ cm. It is seen that in the S1/S3 ratio in the X-X direction, a reduction of up to 52 % is achieved, while S1/S3 in the Y-Y direction is 51 %. In summary, the greatest reduction with the HDRB isolator is generated at point K6, in the X-X direction, at EW displacement, at 52 %.

The HDRB isolator (K6 - corner), in the S1 soil with the earthquake of Ica_2007_NS, shows a $\Delta = 9.74$ cm, in the X-X direction, for the Y-Y direction, with the earthquake of Ica_2007_NS a $\Delta = 10.09$ cm. However, for soil S3 a $\Delta = 37.65$ cm in the X-X direction, and for the Y-Y direction a $\Delta = 39.10$ cm, where the influence between S1/S3 for the X-X direction reaches a reduction percentage of up to 74 % and 74 % in the Y-Y direction.

In the case of point K-26 to the center, for soil S1 the X-X direction a $\Delta = 10.19$ cm and for the Y-Y direction a $\Delta = 10.20$ cm. For soil S3, the X-X direction a $\Delta = 38.20$ cm, and for the Y-Y direction a $\Delta = 39.28$ c. As for the percentage reduction, it reaches 73% in the X-X direction and 74% in the Y-Y direction. In summary, the highest reduction with the HDRB isolator is achieved at point K-6 in both X-X and Y-Y directions, with NS displacement, by 74% respectively.

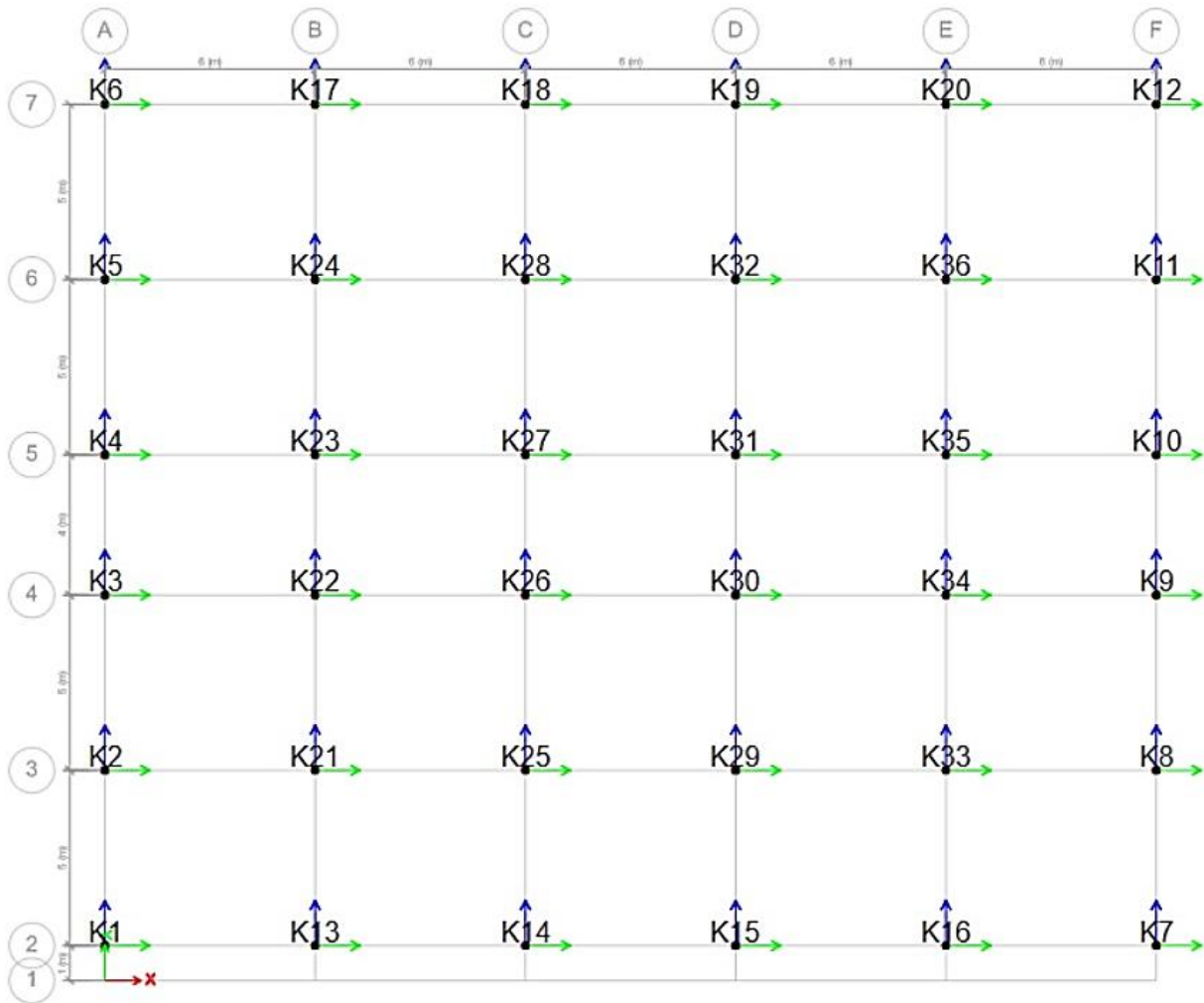


Figure 9. Distribution and analysis of HDRB base isolators

Table 13. Influence S1/S3 - Analysis Isolator_K6_Direction_EW

HYSTERESIS DIAGRAM OF INSULATOR K-6 DIRECTION EW

Description	Soil Type 1		Soil Type 3		Influence	Influence
	Δ Max. X-X	Δ Max. Y-Y	Δ Max. X-X	Δ Max. Y-Y		
Case	cm	cm	cm	cm	%	%
Seism	15.87	16.42	33.17	33.65	52%	51%

Table 14. Influence S1/S3 - Analysis Isolator_K6_Direction_NS

HYSTERESIS DIAGRAM OF INSULATOR K-6 DIRECTION EW

Description	Soil Type 1		Soil Type 1		Influence	Influence
	Δ Max. X-X	Δ Max. Y-Y	Δ Max. X-X	Δ Max. Y-Y		
Case	cm	cm	cm	cm	%	%
Seism	9.73	10.09	37.65	39.10	74%	74%

4.8. Energy Dissipated by HDRB Isolators According to the Simulation on Soil Type S1 and S3

It is important to have information on the magnitude of energy that can be dissipated according to the simulation, using the resources of the Etabs V.20.0.0 *software*. In this sense, the reduction of the stiffness is exposed, and its natural period is increased, thus reducing the acceleration generated by the earthquake. In this way, the seismic isolators, in addition to showing the capacity to dampen the effects of the earthquake, allow a reduction of the coordinates of the elastic spectrum of accelerations. Figures 10 and 11 show the results generated by the simulation in the case of HDRB isolators on S1 and S3-type soil.

Explicitly, this simulation indicates that for the case Ica_2007, the influence on energy dissipation in direction and direction EW_X-X in soil S1 is 82.10 %, while in S3 it is estimated at 84.37 %. Similarly, in EW_Y-Y, 83.75 % is achieved for S1 and 79.87 % for S3. In the NS_X-X direction and direction, it was estimated that for S1 it was 83.68 %, and for S3 it was 78.47 %, while for NS_Y-Y, the percentage of energy dissipation in S1 was 85 % and for S3 79.24 %. Consequently, the values of energy input to the structure and values of dissipation or absorption of such energy by the HDRB high damping isolation devices, allow a percentage estimate of soil type S1/S3 ratio of 75 %. This means that on S1 soil these isolators will make a greater contribution, dissipating a higher percentage of input energy, and strengthening, in addition, the seismic behavior of a type A1 building.

4.9. Discussion

The results obtained are related to the contributions established in a referential manner. First, it has been verified that the safety level of the structure is indeed increased, which improves the structural behavior with the use of anti-seismic elastomeric isolators, as pointed out by Garrido & Fernández-Dávila [29]. These researchers concluded that the isolators can modify the structural behavior in high-impact earthquakes, considerably increasing the lateral displacements and drifts.

In the same way, it was possible to determine the acceleration of the structure that was simulated under the conditions of the 2007 Ica earthquake, something similar to that reported by Bedoya-Zambrano *et al* [24], who used 8 different events. To check the effectiveness, 6 MR magnetorheological dampers were installed to improve the dynamic response in a 96 m high building. This contribution is of great help because it shows that there are modern technology-based means that can cope with the potential effects of an earthquake on urban structures. Finally, the insertion of elastomeric anti-seismic isolators in structures located on S1 soils contributes in a higher proportion in terms of safety compared to the S3 type. This was evidenced by the results of the present study, where these devices are supported by Ahn *et al* [11], who reported a higher shear wave expansion velocity in S1 soil than in S3 soil. Therefore, the implementation of anti-seismic elastomeric isolators effectively contributes to reducing the potentially devastating effects of an earthquake of considerable magnitude.

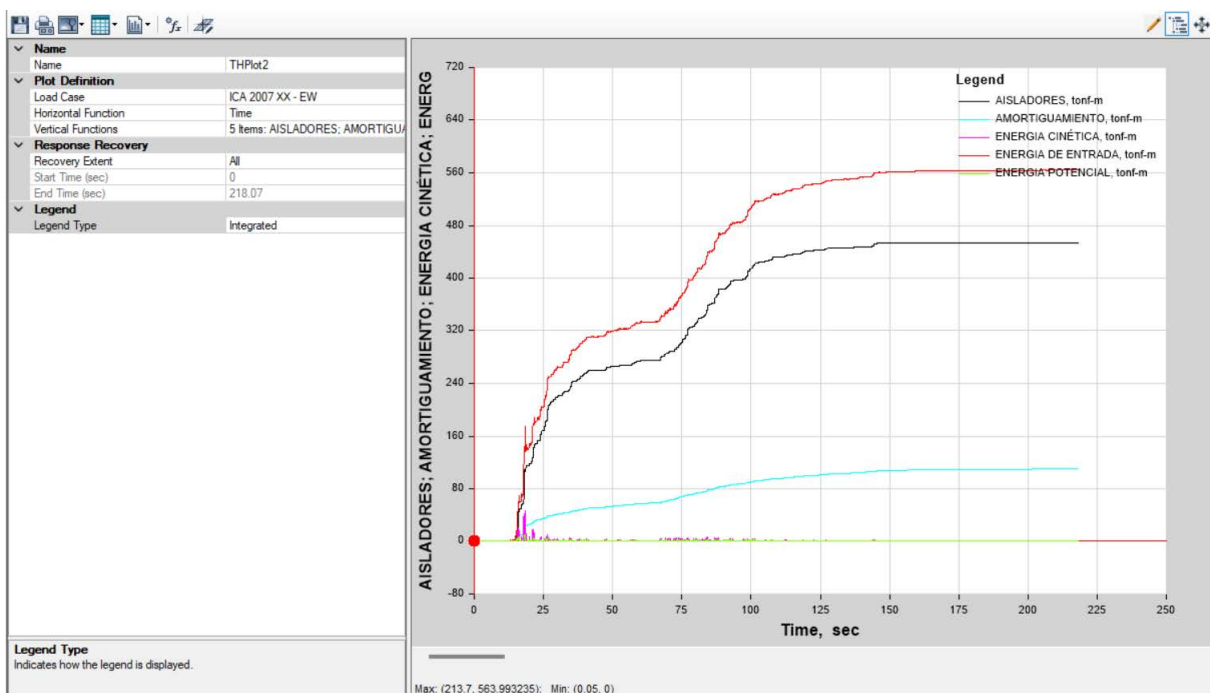


Figure 10. Graphical representation of the energy dissipated by HDRB insulators on soil type S1

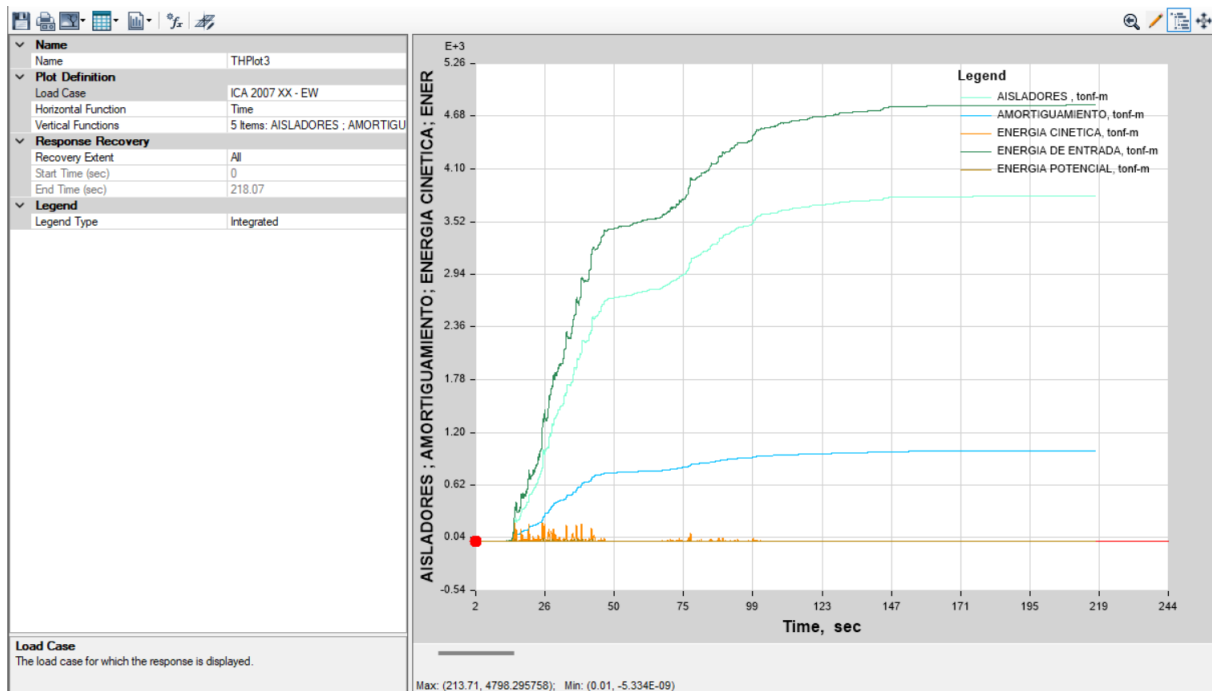


Figure 11. Graphical representation of energy dissipated by HDRB insulators in soil type S3

5. Conclusions

It was determined that after performing the simulation under the conditions specified in the Ica 2007 seismic record, the same magnitude was estimated for soils S1 and S3 for the period of vibration of the building with fixed and insulated base since it is given by the rigidity and weight of the structure. As for the seismic response to shear forces at the base for the insulated and fixed base structure, in the S1 soils with an SMC $R=2$, they were significantly reduced both in the X-X and Y-Y directions. Similarly, the shear forces at the base are decreased for the isolated and fixed-base structure, where the impact of the soil type ratio S1/S3 for the fixed-base version shows an increase of 27%, and for the isolated-base structure, 58% in the analysis in the X-X direction.

The isolated structure on soil type S1 has a maximum drift value of 0.0016 m at the first level. Regarding the importance of the functionality of the isolators, they can significantly dissipate the seismic energy entering the structure.

For soil type S1, energy of 1417.67 Ton/m enters the isolated structure where the HDRB devices absorb 1164.03 Ton/m, thus reducing the input energy to the superstructure by up to 82 % in the X-X direction, while in the Y-Y direction an energy of 1450.58 Ton/m enters, where the HDRB isolators absorb 1214.97 Ton/m, thus reducing its seismic input energy by up to 84 %.

As a result, the values of acceleration reach between 0.1905 g and 0.2529 g in the fixed-base structure. These are decreased by up to 90 % in the X-X direction, and in the Y-Y direction, by up to 92 % concerning the same insulated base for a soil type S1. For the fixed base

structure with soil type S3, the structure is reduced by up to 83 % in the X-X direction, and in the Y-Y direction, by up to 85 % with respect to the same isolated base structure.

Therefore, in the case of an A1 structure with elastomeric isolation with HDRB devices, if an earthquake with similar characteristics to the one in Ica 2007 was to occur, the medical equipment, materials, and infrastructure have a high possibility of not experiencing a high impact damage and will be able to maintain continuous functionality.

Finally, it was specified that the values of energy input to the structure and the values of dissipation or absorption of this energy by the HDRB isolation devices, allow a ratio between S3/S1 soils that reaches values of up to 75%. Consequently, on S1 soil, HDRB isolators will make a better contribution and will dissipate a higher percentage of input energy, strengthening the seismic behavior of a type A1 building.

REFERENCES

- [1] Stepinac, M., Kisicek, T., Renic, E., Hafner, I., Bedon, C, "Methods for the Assessment of Critical Properties in Existing Masonry Structures under Seismic Loads—The ARES Project", Applied Sciences, vol. 10, no. 5, p. 1576, 2020. <https://doi.org/10.3390/app10051576>.
- [2] Owen, JR., Kemp, D., Lebre, E., Svobadova, K., Pérez, G, "Catastrophic tailings dam failures and disaster risk disclosure", International Journal of Disaster Risk Reduction, vol. 42, p. 101361, 2020. <https://doi.org/10.1016/j.ijdr.2019.101361>.

- [3] Zhang, P., Wang, C., Gao, Z., Wang, F, "A review on fracture properties of steel fiber reinforced concrete", *Journal of Building Engineering*, vol. 67, p. 105975, 2023. <https://doi.org/10.1016/j.jobbe.2023.105975>.
- [4] J. Cortés-Pérez, M. Núñez-Fernández, A. Cortés-Pérez, M. Jiménez-Espada, "First application of reinforced concrete in Spain and first European application in bridges: The rehabilitation of the Roman bridge of Alcántara", *Case Studies in Construction Materials*, vol. 19, p. e02350, 2023. <https://doi.org/10.1016/j.cscm.2023.e02350>.
- [5] A. Simon, M. Wilhelmy, R. Klosterhuber, E. Cocuzza, C. Geitner, K. Katzensteiner. "A system for classifying subsolum geological substrates as a basis for describing soil formation", *Catana*, vol. 198, p. 15026, 2021. <https://doi.org/10.1016/j.catana.2020.105026>.
- [6] A. Furtado, H. Rodrigues, A. Arêde, H.A. Varum, "Review of the Performance of Infilled RC Structures in Recent Earthquakes", *Applied Sciences*, vol. 11, no. 13, pp. 58-89, 2021. <https://doi.org/10.3390/app11135889>.
- [7] C. Khong, C. Christopoulos, "Self-centering seismic-resistant structures: Historical overview and state-of-the-art", *Earthquake Spectra*, vol. 38, no. 2, pp. 1321-1356, 2022. <https://doi.org/10.1177/87552930211057581>.
- [8] H. Wang, H. Yang, Y. Feng, B. Jeremi. "Modeling and simulation of earthquake soil structure interaction excited by inclined seismic waves", *Soil Dynamics and Earthquake Engineering*, vol. 46, no. 106720, pp. 1-16, 2021. <https://doi.org/10.1016/j.soildyn.2021.106720>.
- [9] E. Uddin, K. Musab, "Analysis and design of buildings using Revit and ETABS software", *Materials Today: Proceedings*, vol. 65, pp. 1478-1485, 2022. <https://doi.org/10.1016/j.matpr.2022.04.463>.
- [10] R. Divya, K. Murali, "Comparative analysis of behaviour of horizontal and vertical irregular buildings with and without using shear walls by ETABS software", *Materials Today: Proceedings*, vol. 52, pp. 1821-1830, 2022. <https://doi.org/10.1016/j.matpr.2021.11.489>.
- [11] J. Ahn, D. Kwak, H. Kim, "Estimating VS30 at Korean Peninsular seismic observatory stations using HVSR of event records", *Soil Dynamics and Earthquake Engineering*, vol. 146, p. 106650, 2021. <https://doi.org/10.1016/j.soildyn.2021.106650>.
- [12] X. Gao, X. Li, L. Zhao, Y. Kuzyakov, "Shrubs magnify soil phosphorus depletion in Tibetan meadows: Conclusions from C:N:P stoichiometry and deep soil profiles", *Science of the Total Environment*, vol. 785, pp. 147320, 2021. <https://doi.org/10.1016/j.scitotenv.2021.147320>.
- [13] J. de la Cruz, R. Yoctun, "Análisis comparativo del diseño estructural de una edificación regular e irregular de ocho niveles en sistema de pórticos aplicando la norma E.030 2003, 2016 y 2018 diseño sismorresistente en la Ciudad de Lima [Comparative analysis of the structural design of a regular and irregular building of eight levels in a ports system applying standard E.030 2003, 2016 and 2018 seismic resistant design in the city of Lima]", *Gaceta Técnica*, vol. 23, no. 1, pp. 48-71, 2022. <https://doi.org/10.51372/gacetatecnica231.5>.
- [14] S. Ruggieri, A. Fiore, G. Uva, "A New Approach to Predict the Fundamental Period of Vibration for Newly-designed Reinforced Concrete Buildings", *Journal of Earthquake Engineering*, vol. 26, no. 13, pp. 6943-6968, 2021. <https://doi.org/10.1080/13632469.2021.1961929>.
- [15] J. Pineda-Jaimes, C. García-Ubaque, R. Esquivel-Ramírez, "Assessment of Geotechnical Hazard due to Deep Excavations in Bogota Clays: A Contribution for Sustainability in Urban Environments," *Revista Facultad de Ingeniería*, vol. 29, no. 54, pp. 1-26, 2020. <https://doi.org/10.19053/01211129.v29.n54.2020.11373>.
- [16] J. García, H. Scaletti, "Seismic analysis of underground structures: influence of the soil type, the relative stiffness and seismic intensity", *TECNIA*, vol. 32, no. 02, pp. 185-198, 2022. DOI: <https://doi.org/10.21754/tecnia.v32i2.1430>.
- [17] Y. Chua, J. Richard, S. Pang, "Modelling of connections and lateral behavior of high-rise modular steel buildings", *Journal of Constructional Steel Research*, vol. 166, p. 105901, 2020. <https://doi.org/10.1016/j.jcsr.2019.105901>.
- [18] A. Lacey, W. Chen, H. Hao, K. Bi, "Effect of inter-module connection stiffness on structural response of a modular steel building subjected to wind and earthquake load", *Engineering Structures*, vol. 213, pp. 110628, 2020. <https://doi.org/10.1016/j.engstruct.2020.110628>.
- [19] G. Pianese, N. Van Engelen, H. Toopchi-Nezhad, G. Milami, "High-damping fiber-reinforced elastomeric seismic isolator in different boundary conditions: An experimental insight", *Engineering Structures*, vol. 300, p. 117199, 2024. <https://doi.org/10.1016/j.engstruct.2023.117199>.
- [20] D. Losanno, D. De Domenico, I. Madera-Sierra, "Experimental testing of full-scale fiber reinforced elastomeric isolators (FREIs) in unbounded configuration", *Engineering Structures*, vol. 260, pp. 114234, 2022. <https://doi.org/10.1016/j.engstruct.2022.114234>.
- [21] E. Ghorbi, H. Toopchi-Nezhad, "Annular fiber-reinforced elastomeric bearings for seismic isolation of lightweight structures", *Soil Dynamics and Earthquake Engineering*, vol. 166, pp. 107764, 2023. <https://doi.org/10.1016/j.soildyn.2023.107764>.
- [22] F. Mazza, M. Mazza, "Influence of Elastomeric Bearings in Tension on the Seismic Performance of Base-Isolated R.C. Buildings", *Applied Sciences*, vol. 11, no. 1, p. 82, 2021. <https://doi.org/10.3390/app11010082>.
- [23] D. Coffetti, E. Crotti, G. Gazzaniga, R. Gottardo, T. Pastore, L. Coppola, "Protection of Concrete Structures: Performance Analysis of Different Commercial Products and Systems", *Materials*, vol. 14, no. 13, p. 3719, 2021. <https://doi.org/10.3390/ma14133719>.
- [24] D. Bedoya-Zambrano, L. Lara-Valencia, J. Blandón-Valencia, "Desarrollo de un algoritmo híbrido de control de amortiguadores magnetorreológicos para optimizar la respuesta dinámica en pórticos [Development of a hybrid control algorithm for magnetorheological dampers to optimize the dynamic response in frames]", *Entramado*, vol. 20, nro. 1, pp. 1-25, 2024. <https://doi.org/10.18041/1900-3803/entramado.1.10270>.
- [25] R. Noggle, N. Van Engelen, "Stress distributions of infinite strip steel reinforced elastomeric isolators with a rubber core", *Engineering Structures*, vol. 285, p. 116033, 2023. <https://doi.org/10.1016/j.engstruct.2023.116033>.

- [26] C. Yenidogan. "Earthquake-Resilient Design of Seismically Isolated Buildings: A Review of Technology". *Vibration*, vol. 4, pp. 602–647, 2021. <https://doi.org/10.3390/vibration4030035>
- [27] J. Amado, P. Ross, N. Sanches, J. Pinto, J. Dutra. Evaluation of elastomeric heat shielding materials as insulators for solid propellant rocket motors: A short review. *Open Chemistry*, vol. 18, no. 1, pp. 1452-1467, 2020. <https://doi.org/10.1515/chem-2020-0182>
- [28] L. Yang, Z. Ou, G. Jiang, "Research Progress of Elastomer Materials and Application of Elastomers in Drilling Fluid. *Polymers*, vol. 15, no. 918, 2023. <https://doi.org/10.3390/polym15040918>
- [29] C. Garrido, V. Fernández-Dávila, "Comportamiento sísmico de edificios irregulares en planta considerando sistemas de aislamiento con excentricidad de rigidez [Seismic behavior of irregular buildings in plan considering isolation systems with stiffness eccentricity]", *Ingeniería*, vol. 34, no. 2, pp. 9–20, 2024. <https://doi.org/10.15517/ri.v34i2.55859>
- [30] M. Rafik, B. Abdelhak, "The Use of Seismic Isolators to Improve Building Performance", *Journal of Civil Engineering*, vol. 18, no. 1, pp. 1-11, 2023. <https://doi.org/10.2478/sspjce-2023-0004>
- [31] B. Cagua, R. Aguiar, J. Pilatasig, D. Mora, "Acoplamiento de Opensees con Ceinci-Lab para análisis estático no lineal. Primera parte: Reforzamiento sísmico con diagonales de acero [Coupling Opensees with Ceinci-Lab to Perform Non-Linear Static Analysis. First Part: Seismic Reinforcement with Steel Braces]", *Revista Internacional de Ingeniería de Estructuras*, vol. 25, no. 3, pp. 367-420, 2020. <http://doi.org/10.24133/riie.v25i3.1691>.
- [32] A.H. Delingol, E.M. Guneyisi. "Effect of Using High Damping Rubber Bearings for Seismic Isolation of the Buildings", *International Journal of Steel Structures*, vol. 21, no. 5, pp. 1698-1722, 2021. DOI: <http://doi.org/10.1007/s13296-021-00530-w>
- [33] B. Lovery, M. Chlieh, E. Norabuena, J. C. Villegas-Lanza, M. Radiguet, N. Cotte, A. Tsapong-Tsague, W. Quiroz, C. Sierra Farfán, M. Simons, J. M. Nocquet, H. Tavera, A. Socquet, "Heterogeneous Locking and Earthquake Potential on the South Peru Megathrust From Dense GNSS Network", *Journal of Geophysical Research: Solid Earth*, vol. 129, no. 2, e2023JB027114, 2024. <https://doi.org/10.1029/2023JB027114>
- [34] J.C. Raj, M.V. Kumar. "Performance evaluation of eco-friendly scrap tyre base isolation technology in distinct construction quality RC framed buildings located in seismic risk zone", *Sustainable Energy Technologies and Assessments*, vol. 53, p. 102511, 2022. <https://doi.org/10.1016/j.seta.2022.102511>
- [35] E.U. Syed, K.M. Manzoor. "Analysis and design of buildings using Revit and ETABS software", *Materials Today: Proceedings*, vol. 65, pp. 1478-1485, 2022. <https://doi.org/10.1016/j.matpr.2022.04.463>.
- [36] A. Gerges, M.C. Porcu, J.C. Vielma, "Contribution to Facilitate the Seismic Design in Lebanon Using Short-Length Spectrum-Consistent Earthquakes". *Applied Sciences*, vol. 13, no. 24, p. 12990, 2023. <https://doi.org/10.3390/app132412990>.
- [37] G. Villarreal, M. Cerna, C. Espinoza, "Seismic interaction of soil-structure in buildings with limited ductility walls on foundation plates", *Revista Internacional de Ingeniería de Estructuras*, vol. 26, no. 1, pp. 153-178, 2021. <http://doi.org/10.24133/riie.v26i1.1967>.
- [38] A. Tena, D. Parra, "Diseño sísmico resiliente de un edificio esbelto de acero conforme a las recomendaciones de aislamiento sísmico de México [Resilient Seismic Design of a Slender Steel Building According to the Seismic Isolation Guidelines of Mexico]", *Revista Internacional De Ingeniería De Estructuras*, vol. 29, no. 1, pp. 1-36, 2024. <https://doi.org/10.24133/csp8jk58>
- [39] Norma Técnica E-31. Aislamiento Sísmico del Reglamento Nacional de Edificaciones. *Diario El Peruano. Normas Legales*, pp. 65-84. https://cdn-web.construccion.org/normas/rne2012/rne2006/files/titulo3/02_E/2019_E031_DS-03-0-2019-VIVIENDA.pdf